

## BEHAVIOUR AND DESIGN OF CORNER OR L-JOINTS IN SC WALLS

Jungil Seo<sup>1</sup> and Amit H. Varma<sup>2</sup>

<sup>1</sup> Research Engineer, Purdue University, USA (seo2@purdue.edu)

<sup>2</sup> Professor, Lyles School of Civil Engineering, Purdue University, USA

### ABSTRACT

A large scale SC wall-to-wall corner or L-joint specimen was tested under cyclic loading until failure to investigate the fundamental joint shear behaviour of the specimen. The test specimen was designed to fail with joint shear failure prior to flexural yielding of SC walls. The test results included the joint shear – displacement ( $V_{js} - \Delta$ ), joint shear – shear strain ( $V_{js} - \gamma$ ), and joint shear – steel strain ( $V_{js} - \epsilon_s$ ) responses of the specimen along with observations of concrete cracking and crushing in the joint region. The results and observations were reviewed to determine the joint shear strength and governing failure mode. The experimentally measured joint shear strength of the specimen was compared with the ACI 349-06 code equation for RC calculating the joint shear strength of reinforced concrete beam-to-column joints. A detailed nonlinear finite element model was developed to gain additional insights into the observed behaviour. The model was benchmarked using the experimental results. The experimental and analytical results were compared with ACI 349-06 code provisions for calculating the joint shear strength of reinforced concrete beam-to-column joints.

### INTRODUCTION

Steel-plate composite (SC) walls have been of interest for the containment internal structures (CIS) of the third generation nuclear power plants and small modular reactors (SMR). The interest in SC walls stems from their superb structural performance investigated for past two decades and construction efficiency evidenced by recent construction of the AP1000® nuclear power plants in Sanmen, China, and in the US in Vogtle, Georgia and in V.C. Summer in South Carolina.

SC walls in the CIS typically consist of two steel faceplates (made from A36 or A572 Gr. 50) on both exterior surfaces with concrete ( $f'_c = 4,000 - 6,000$  psi.) filled between them. The two faceplates are connected to each other using structural elements such as tie bars, angles, channels, or other structural fasteners. They are also anchored to the concrete infill using stud anchors that are welded on the interior surfaces close enough to prevent local buckling of the steel faceplates. In the CIS SC walls often form joints (T or L) where two or three SC walls join together.

Designing SC wall-to-wall joints is challenging because: (i) there are no clear performance requirements specified by any code or standard, and (ii) there are no pre-qualified or pre-developed, and tested connections for engineers to select from. With the lack of information, full-strength connection design can be used for designing SC wall-to-wall joints. With this design philosophy, the joint region is designed to be stronger than the connected SC walls. The connected SC walls fail before the joint region fails by forming plastic hinges, where energy dissipation occurs through inelasticity of them. To design the joint region with adequate shear strength to resist the demands placed on it, it is important to estimate the joint shear strength of the region.

## BACKGROUND AND OBJECTIVES

Seo (2015) conducted an experimental study to investigate the joint shear behaviour and joint shear strength of SC wall-to-wall T joints. The test parameters included the shear reinforcement ratio ( $\rho_t$ ) and stud anchor layout in the joint region. The author also evaluated the applicability of the equation for RC beam-column joint strength (given in Section 21.5.3 of ACI 349-06 (2006)) to estimating the joint shear strength of SC wall-to-wall T joints. The equation is shown in Equation 1. In the equation, the  $\gamma$  value of 12 for RC beam-column joints (Case A and Type B in ACI 352R-02) with one column framing into the joint was selected for SC wall-to-wall T joints. The effective cross-sectional area within a joint ( $A_j$ ) is calculated using the effective joint widths and depths. For the SC wall-to-wall joints, the joint area ( $A_j$ ) is calculated as the total cross sectional area of the concrete infill within the joint region subjected to horizontal or vertical shear.

Based on the experimental results, the author concluded that (i) the effects of the shear reinforcement ratio ( $\rho_t$ ) and stud anchor layout in the joint region are not significant and (ii) the ACI 349-06 (2006) code equation can be used to estimate the joint shear strength of SC wall-to-wall T joints with  $\gamma$  value of 12. However, the author conducted an experimental study on SC wall-to-wall T joints only. Therefore, fundamental experimental and analytical studies on SC wall-to-wall L joints are need.

Case B3 of Type 2 connections in ACI 352R-02, where one column frames into the joint is recommended for SC wall-to-wall L joints, which consists of a discontinuous SC wall connected to a discontinuous SC wall forming the L-joint. The joint region is confined on less than three vertical faces. This is particularly the case for SC wall L-joints subjected to accidental thermal loading, which causes steel expansion and concrete cracking due to elevated temperatures. This minimizes the potential confinement on horizontal faces due to the self-weight of SC walls. Therefore, the  $\gamma$  value of 8 is selected for SC wall L-joints in this study.

$$V_n = \gamma \sqrt{f'_c} A_j \quad (1)$$

The objectives of this study are (i) to investigate the joint shear behaviour of SC wall-to-wall L joints, (ii) to determine the joint shear strength and governing failure mode of SC wall-to-wall L joints, and (iii) to evaluate the applicability and conservatism of the ACI 349-06 (2006) code equation for estimating the joint shear strength of SC wall-to-wall L joints. In this paper, the results of experimental and analytical investigations are to be presented.

## EXPERIMENTAL INVESTIGATION

A large-scale test was conducted on SC wall-to-wall L joint connection. The test specimen was designed to undergo joint shear failure prior to flexural yielding of the connected SC walls. This was done by thickening the faceplates. Details of the test specimen are presented in Table 1. The test specimen is briefly illustrated in Figure 2. As presented and shown, the specimen had two SC walls (60 in. long and 30 in. deep by 15 in. wide in cross section) connected to the joint region. The faceplate thickness ( $t_p$ ) was  $\frac{3}{4}$  in. The faceplates were connected to each other using steel tie plates ( $3\frac{3}{4} \times \frac{5}{16}$  in.) welded on the interior surface of the steel faceplates at every 15 in. Stud anchors ( $\frac{1}{2}$  in. diameter and 4 in. long) were also welded on the faceplates at every 5 in. resulting in a plate slenderness ratio ( $s/t_p$ ) of 6.67. No shear reinforcement was provided in the joint region. However, a group of stud anchors having adequate shear resistance to demand on them was welded on interior surfaces of the region.

The measured steel yield strengths ( $F_y$ ) were 59.1 ksi for faceplates and 62.7 ksi for tie plates. The measured steel tensile strengths ( $F_u$ ) were 79.6 ksi for faceplates, 73.5 ksi for tie plates, and 80.9 ksi for stud anchors. The measured concrete compressive strength ( $f'_c$ ) was 5,900 psi.

Table 1: Geometry and material properties of test specimen

Specimen	Geometry					Material Property					
	$l$ , in.	$T$ , in.	$t_p$ , in.	$w$ , in.	No. of tie plates	Concrete	Faceplate		Tie plate		Stud
						$f'_c$ , psi	$F_y$ , ksi	$F_u$ , ksi	$F_y$ , ksi	$F_u$ , ksi	$F_u$ , ksi
JS-T0-F-L	60	30	0.75	15	0	5,900	59.1	79.6	62.7	73.5	80.9

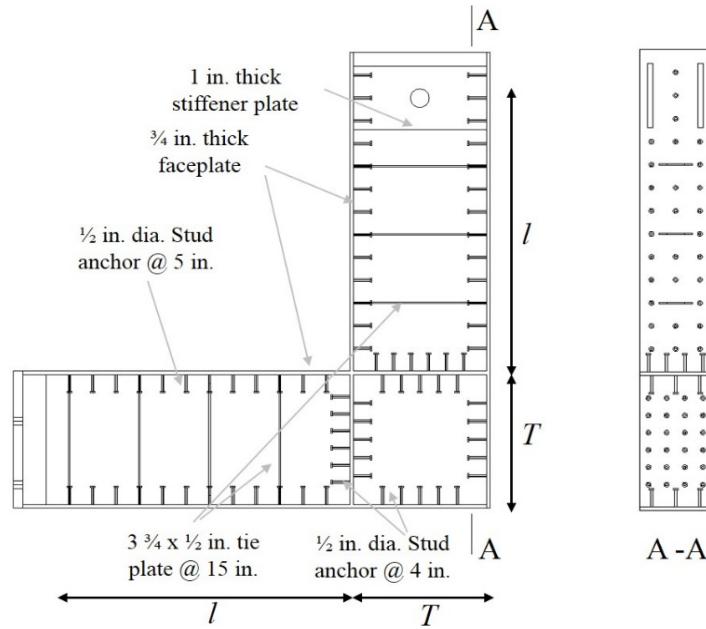


Figure 1. Schematic view of test specimen

### Test Setup and Loading Protocol

The test specimen was placed in the test setup as illustrated in Figure 2 (a). The specimen was connected to a steel wall box using a steel link and pin supports as shown in the figure. The east end was connected to the steel link using four 1.5 in. diameter threaded rods and clevises. Two pin connections were established using two 4 in. diameter steel rods to provide the roller boundary condition. The south end was connected to the pin support using a 4 in. diameter steel rod. The east end was also connected to a 250 kip capacity hydraulic actuator using four 1.5 in. diameter threaded rods and clevises.

The lateral load ( $H$ ) was applied to the east end of the specimen. The applied loading increased cyclically as shown in Figure 2 (b). In the figure,  $H_n$  is the lateral load corresponding to the joint shear strength calculated using the ACI 349-06 (2006) equation ( $\gamma = 8$ ) and measured concrete compressive strength ( $f'_c$ ) on the day of test ( $V_{njs}^{ACI}$ ). The specimen was subjected to cyclic loading under both load control and displacement control. As shown in the figure, the elastic cycles were conducted under load control at lateral load levels of 0.25, 0.5, and 0.75 $H_n$ . In the figure,  $\Delta_y$  is the projected displacement at  $H_n$ . Since the test specimens were expected to fail in a non-ductile manner, the displacement at the first cycle of 0.75 $H_n$

was used to calculate  $\Delta_y$ . The displacement at  $0.75H_n$  was multiplied by 1.33 to estimate  $\Delta_y$ . Additional displacement cycles with different amplitudes ( $1.25\Delta_y$ ,  $1.50\Delta_y$ ,  $2.00\Delta_y$ , and  $2.50\Delta_y$ ) were in the loading protocol.

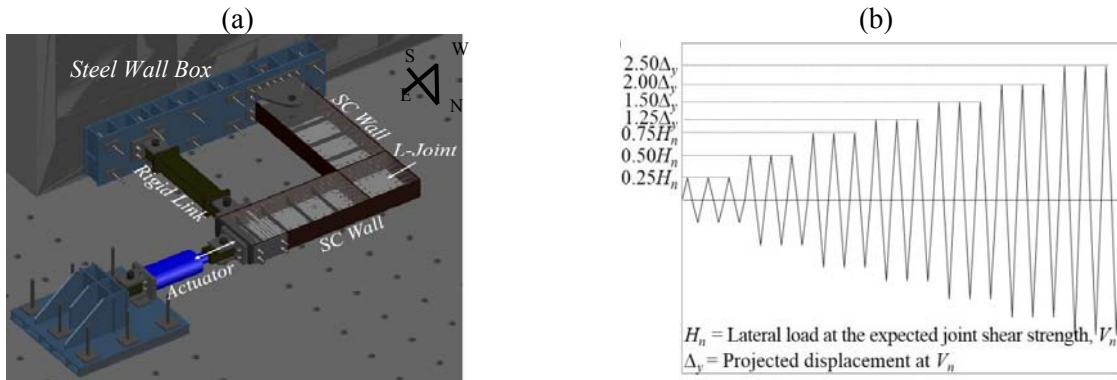


Figure 2. (a) 3D isometric view of test setup and (b) loading protocol

### Joint Shear

Figure 3 (a) shows how the applied lateral load ( $H$ ) is transferred to the supports along with the bending moments and shear forces in the connected SC walls. Shear forces are generated by the bending moments and shear forces in the joint region and they are illustrated in Figure 3 (b). Two identical joint shear force ( $V_{js}$ ) terms are the resultants of (i) the shear forces ( $H$  and  $R_y$ ) acting on the joint surfaces, and (ii) the decomposed tension and compression forces from the bending moments acting on each side. The joint shear force term is shown in Equation 2. In the equation,  $j$  is the distance between the resultant compression force and tension force due to bending moments. The force equilibrium equation developed by Varma et al. (2011) for the cracked-transformed flexural section can be used to calculate  $j$ , however, its value is very close to 0.92 for all practical purposes.

$$V_{js} = H \left( \frac{l}{jT} - \frac{1}{2} \right) \quad (2)$$

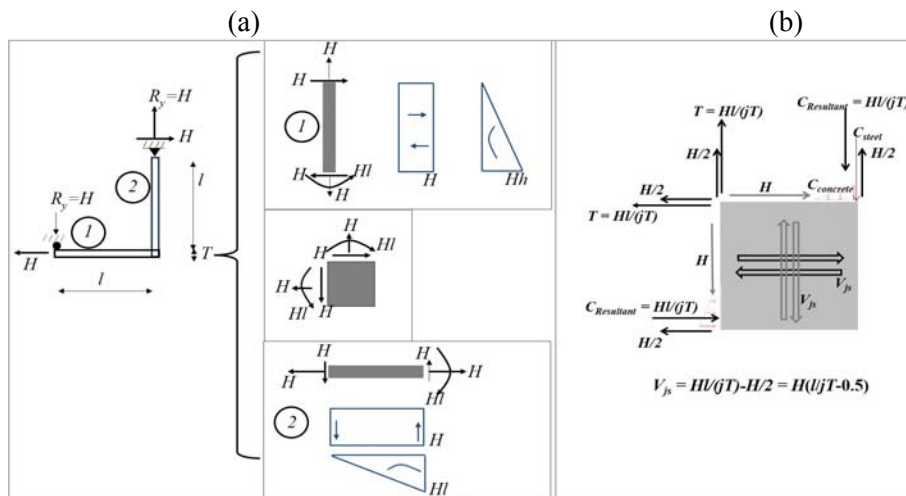


Figure 3. (a) Force transfer mechanism and (b) force transfer mechanism focused in the joint region

## Instrumentation

The data at interest was the applied lateral load ( $H$ ), displacements, steel longitudinal strains, and shear strains of the joint region. They were measured using a calibrated load cell, displacement transducers, strain gauges, and OPTOTRAK targets as illustrated in Figure 4. The applied lateral load ( $H$ ) was measured using a calibrated load cell which was installed to the actuator. Displacements was measured using string potentiometers (SP1 – SP5). The displacements at the pin and roller supports were also measured using 1 in. stroke displacement transducers (N5 and N6). The steel longitudinal strains in the steel diaphragm plates, steel tie plates, and steel headed studs were measured using electrical-resistance strain gauges (SG) that were installed prior to casting. Additionally, uniaxial strains in the steel faceplates were measured using strain gauges that were installed after casting. Twenty-five OPTOTRAK targets were used to measure the displacement field of the joint region as shown in Figure 4(b).

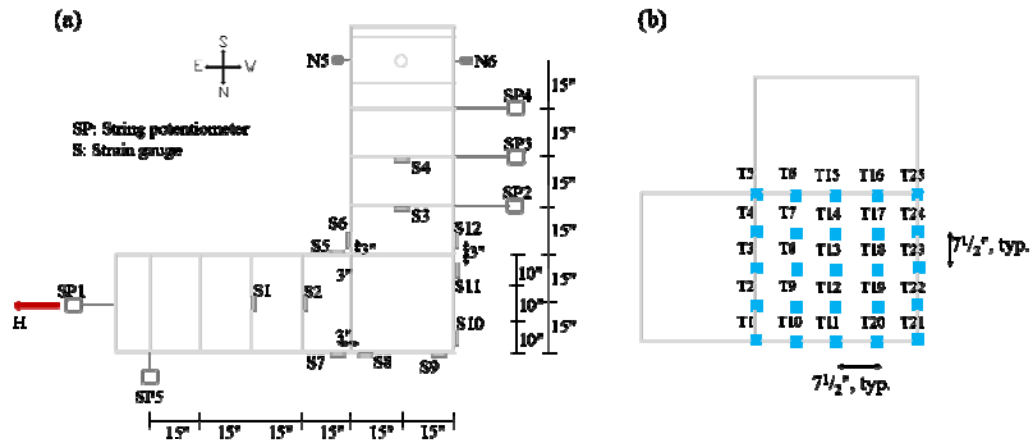


Figure 4. Instrumentation layout: (a) string potentiometer and strain gauge and (b) OPTOTRAK target layout

## Test Results

The experimentally measured joint shear - displacement response at the loading point (SP1) is shown in Figure 5 (a). The first concrete crack occurred in the connected SC walls at  $V_{js}$  of about 67 kips. After the concrete crack occurrence, the specimen exhibited a nearly elastic response up to  $V_{js}$  of 201 kips (about 76.5 % of  $V_{js}^{ACI}$ ). The stiffness of the specimen started to degrade during cycles with displacement control. Concrete in the joint region underwent significant cracking during the cycles and the specimen reached its ultimate strength 261.7 kips in the pull direction (290.3 kips in the push direction).

The experimentally measured joint shear – shear strain response in the joint region is shown in Figure 5 (b). The specimen exhibited a linear response up to the first concrete crack occurrence ( $V_{js} = 134$  kips) in the joint region. Shear strain increased radically with the crack. The stiffness degraded with additional concrete cracking in the joint region and the specimen failed with joint shear failure. The shear strain at the failure was -0.0071.

Damage initiated with concrete shear cracking in both connected the SC walls and joint region. However, concrete cracking in the connected SC walls remained small (crack width < 0.03 in.) throughout the test. The joint region underwent significant damage with (i) extensive concrete cracking, (ii) spalling of the concrete in the out-of-plane direction, and (iii) yielding of steel diaphragm plates. The measured joint shear strength (261.7 kips) is lower than the joint shear strength computed using the ACI 349-06 (2006) code equation ( $V_{js}^{ACI}$ ) by 0.8 kips. The test results are summarized in Table 2.

Table 2: Summary of experimental results

Specimen	Ultimate joint shear, kips	Shear strain at the ultimate joint shear	Governing failure mode	Event order in the Joint region
JS-T0-F-L	261.7 (-) 290.3 (+)	- 0.0071 (-) 0.0089 (+)	Joint Shear Failure	Concrete crack ↓ Extensive concrete cracking ↓ Yielding of diaphragm plates

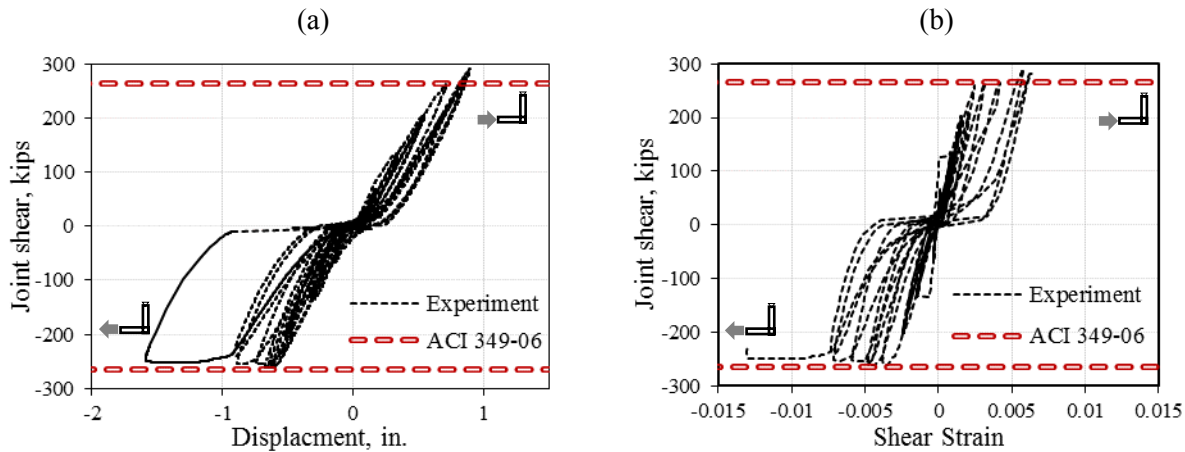


Figure 5. Experimental results: (a)  $V_{js} - \Delta$  response and (b)  $V_{js} - \gamma$  response

## ANALYTICAL INVESTIGATION

Three-dimensional (3-D) finite element method (FEM) model was developed and analysed to gain additional insight into the joint shear behaviour in SC wall-to-wall L joint test specimen. A commercially available analysis program, ABAQUS (2011), was used for the analysis because it had the required nonlinear inelastic analysis capabilities. The analysis results in terms of (i) the joint shear force - displacement ( $V_{js} - \Delta$ ) response and (ii) the joint shear force - shear strain ( $V_{js} - \gamma$ ) response were reviewed and compared with corresponding test results.

### *Analysis Approach*

The steel faceplates and steel tie plates were modelled with shell elements since their thickness ( $t_p = 0.75$  in.) is significantly smaller than the SC wall thickness ( $T = 30$  in.) and width ( $w = 15$  in.). Four-node shell element with reduced integration (S4R) was selected. The element with reduced integration was selected to facilitate convergence and clear understanding of plasticity at the material points. The concrete infill was modelled using eight-node solid elements with reduced integration (C3D8R). The C3D8R element is preferred for performing nonlinear inelastic analysis involving inelastic strains, plasticity, or even cracking at the integration points. The steel stud anchors were modelled using quadratic Timoshenko beam elements (B32). Timoshenko beams allow transverse shear deformation, and the cross-section may not necessarily remain normal to the beam axis.

The interfacial shear behaviour between the steel faceplates and concrete infill was simulated using a three-dimensional, axisymmetric type of connector element (CONN3D2). They are also referred as connector elements. The connector elements model discrete physical connections between deformable or rigid bodies. The CONN3D2 elements have 2 nodes. The position (location, orientation) and motion (displacement etc.) of the second node on the element are measured relative to the first node. The connector elements reduced the complexity of modelling the actual details of the steel headed studs and its embedded interaction with concrete and welded interaction with the steel plate.

Nonlinear load-slip curve proposed by Ollgaard et al. (1971) was input as the relative motion behaviour. This relationship is presented as Equations 3 and 4. In the equations,  $A_{stud}$  is cross-sectional area of a steel headed stud,  $F_u$  is the ultimate strength of a steel headed stud,  $f'_c$  is the compressive strength, and  $E_c$  is elastic modulus of concrete.

$$Q = Q_u \left(1 - e^{-18\Delta}\right)^{\frac{2}{5}} \quad (3)$$

$$Q_u = \min \left( A_{stud} F_{u,stud}, 0.5 A_{stud} \sqrt{f'_c E_c} \right) \quad (4)$$

The idealized uniaxial stress-strain curve was idealized based on reviewing or comparing with the strain hardening portion of the experimentally measured stress-strain curve. The idealized curve is shown in Figure 6(a). The concrete elastic fracture (CEF) model built in ABAQUS (2010) was used to represent the complex behaviour of concrete in tension and shear. The CEF model assumes elastic behaviour in compression. In tension, it uses a brittle fracture model with oriented damaged elasticity concepts to model smeared cracking. It has anisotropic damage rules, and can be used only with dynamic explicit analyses. The post-peak behaviour of the concrete infill was defined using the equations for plain concrete provided in CEB-FIP model code (2010). The behaviour is shown in Figure 6(b). The finite concrete elements that have lost their load carrying capabilities were removed from the mesh to increase the model stability. The element removal also gives a reasonable sense of the potential crack pattern that would be seen in the experiment.

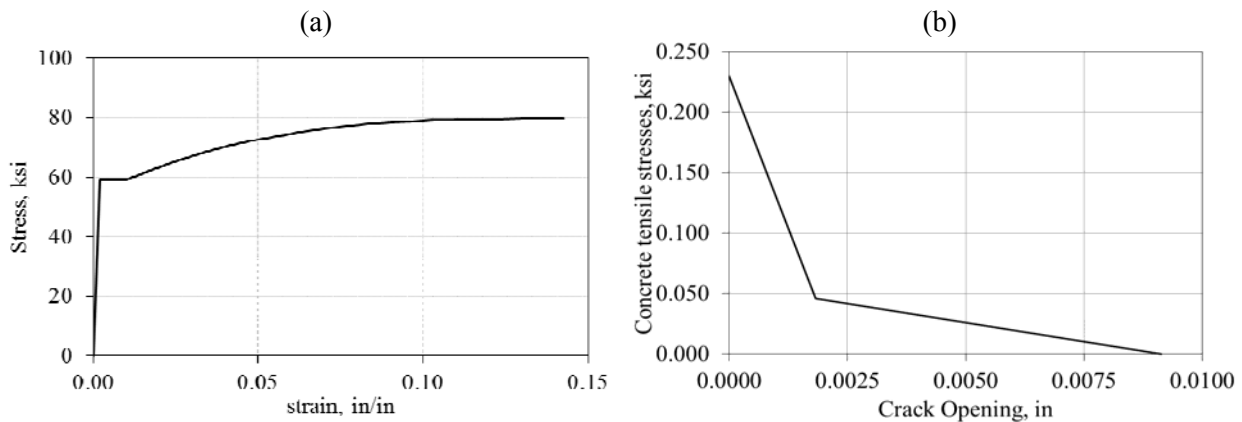


Figure 6. Material properties: (a) idealized steel stress – strain curve and (b) concrete post peak behaviour

### Analysis Results

The analytically predicted joint shear force – displacement ( $V_{js} - \Delta$ ) response and joint shear force – shear strain ( $V_{js} - \gamma$ ) response in the joint region for Specimen JS-T0-F-L are shown in Figure 7. As shown, concrete cracking first occurred in the joint region at  $V_{js}$  of 165 kips. The stiffness started degrading with

additional concrete cracks in both the connected SC walls and the joint region. Concrete finite elements in the joint region underwent significant deformation and started being deleted at  $V_{js}$  of 282.4 kips. More concrete finite elements were deleted and steel finite elements (steel faceplates and diaphragm plates) near the joint region started yielding. It is obvious that the governing failure mode was joint shear failure. The analytically predicted ultimate joint shear strength was 292.3 kips and its corresponding strain was 0.011. The predicted strength was about 10 % greater than the experimental measured strength and joint shear strength calculated using the ACI 349-06 (2006) equation.

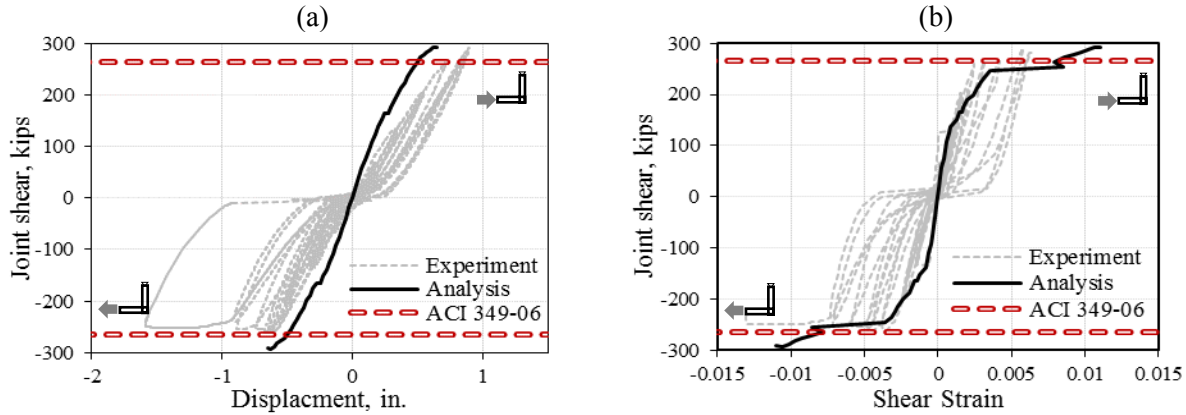


Figure 7. Analytical results: (a)  $V_{js} - \Delta$  response and (b)  $V_{js} - \gamma$  response

Figure 8 shows analytically predicted stress and strain distribution. Figure 8(a) shows maximum principal strain contour plots of the concrete at the ultimate joint shear force. Maximum principal strains greater than 0.003 are shown in grey. Extensive cracking is observed in the joint region. Figure 8(b) shows the minimum principal stress contour plots of the concrete. Minimum principal stresses less than -5,900 psi are shown in black. It illustrates the formation of the concrete compressive strut in the joint region. Figure 8(c) shows the equivalent plastic strain (PEEQ) contour in the steel faceplates. Any colour other than blue indicates yielding. Yielding of the tie bar finite elements was observed. The analytically predicted crack formation in the joint at the ultimate joint shear force is shown in Figure 9(a). The predicted crack formation matches favourably with the experimental observed crack formation shown in Figure 9(b).

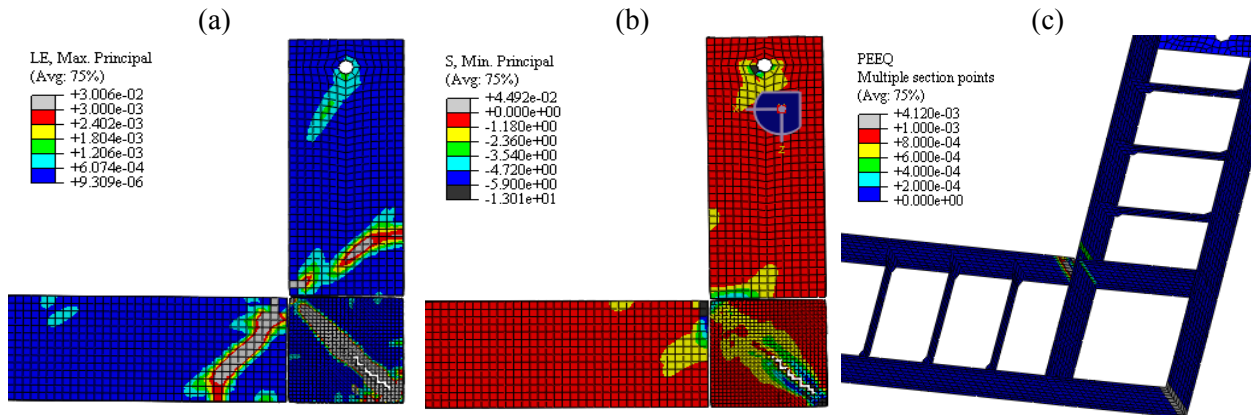


Figure 8. (a) Maximum principal strain distribution in concrete, (b) – Minimum principal stress distribution in concrete, and (c) – PEEQ distribution in steel faceplates and tie bars at ultimate joint shear force

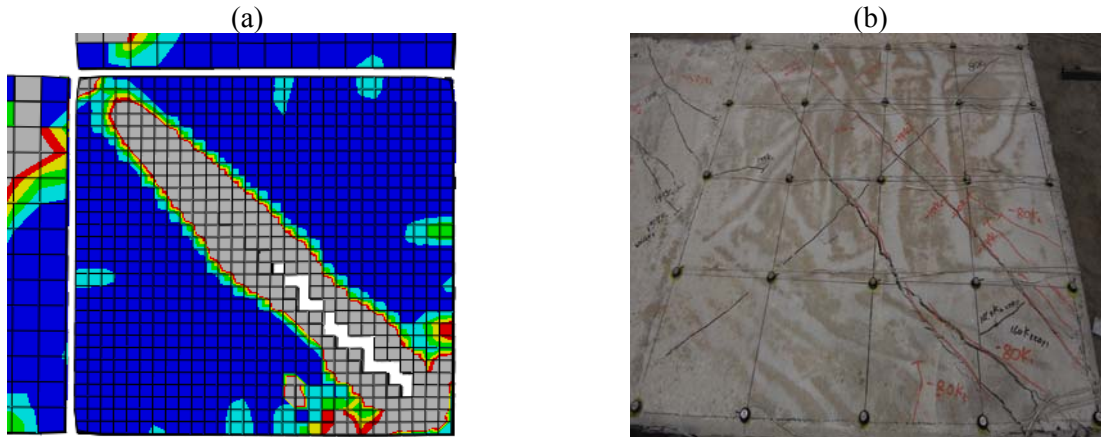


Figure 9. Concrete crack pattern in the joint region at ultimate strength: (a) FE analysis and (b) experiment

## CONCLUSION

Experimental and analytical investigations were conducted to evaluate: (i) the joint shear behaviour and strength of SC wall-to-wall L joints, and (ii) the applicability and conservatism of the ACI 349-06 Section 21.5.3 RC beam-column joint shear strength equation with  $\gamma$  value equal to 8 for estimating the joint shear strength of SC wall L-joints.

One large scale joint shear test was conducted to investigate the fundamental joint shear behaviour of SC wall-to-wall L joint. The test was conducted in a uniquely designed test-setup providing pin and roller boundary conditions and cyclic lateral loading. The experimentally measured responses including joint shear force - displacement responses, and the joint shear force - shear strain, and joint shear force - strain were reviewed to verify the governing failure mode. Three-dimensional (3-D) finite element method (FEM) models were also developed and analysed to predict the joint shear behaviour and strength of the SC wall-to-wall L joint specimen. The experimentally measured and analytically predicted joint shear strengths were compared with joint shear strength calculated using the ACI 349-06 (2006) equation for RC beam-column joint shear strength with measured material properties.

The results from experimental and analytical investigations indicate that:

- The test specimen failed with the joint shear failure mode as designed.
- The experimentally measured joint shear strength of SC wall-to-wall L joint specimen (261.7 kips) was lower than the joint shear strength computed using the ACI 349-06 (2006) code equation by 0.8 kips.
- The analytically predicted joint shear strength of SC wall-to-wall L joint specimen (292.3 kips) was greater than the joint shear strength computed using the ACI 349-06 (2006) code equation by approximately 10 %.
- The ACI 349-06 (2006) code equation is applicable for estimating the joint shear strength of SC wall-to-wall L joints with  $\gamma$  of 8.

## REFERENCES

ACI 349 (2006). "Code Requirements for Nuclear Safety-Related Concrete Structures and Commentary," American Concrete Institute, Farmington Hills, MI

- Seo, J. (2014). *Design of Steel Concrete Composite Wall-to-Wall Joints for Safety-Related Nuclear Facilities*. PhD dissertation, Purdue University
- Joint ACI-ASCE Committee 352. (2002). "Recommendations for Design of Beam-Column Joints in Monolithic Reinforced Concrete Structures (ACI 352R-02)," American Concrete Institute, Farmington Hills, Mich.
- Varma, A.H., Malushte, S.R., Sener, K.C., Booth, P.N., Coogler, K. (2011) "Steel-Plate Composite (SC) Walls: Analysis and Design Including Thermal Effects", Trans. of the Internal Assoc. for Struct. Mech. in Reactor Tech. Conf., SMiRT-21, Paper No. 761, New Delhi, India
- ABAQUS (2011). *ABAQUS/Standard Version 6.10 User's Manuals: Volume I-III*, Hibbitt, Karlsson, and Sorenson Inc., Pawtucket, RI.
- Ollgaard, J.G., Slutter, R.G., and Fisher, J.W. (1971) "Shear Strength of Stud Connectors in Lightweight and Normal-weight Concrete", Engineering Journal – American Institute of Steel Construction, Inc.
- Model Code 2010, "First Complete Draft", fib bulletins 55 and 56, International Federation for Structural Concrete (fib), ISBN 978-2-88394-095-6 and ISBN 978-2- 88394-096-3